ENGINEER - Vol. LVII, No. 04, pp. [67-78], 2024

DOI: https://doi.org/10.4038/engineer.v57i4.7667

Infrared Image-Based Condition Assessment of 33kV SIR Housed ZnO Surge Arresters

R.S.Illesinghe,N.N.K.Paranavithana,M.A.R.M. Fernando and W.L.Abeygunasekara

Abstract: Lightning surge arresters are key components for the protection and reliability of power systems. During service, surge arresters are aged by deteriorating their properties. It is important to monitor conditions periodically in order to avoid failures of power apparatus. This study proposes an online-based condition monitoring method for surge arresters using principal component analysis (PCA), support vector machine (SVM) and thermal image processing of infrared images captured from 46 energized 33kV lightning surge arresters belonging to Ceylon Electricity Board (CEB). Field-energized aged arresters (18 samples), laboratory-tested aged arresters (27 samples) and a brand-new arrester were taken for the investigation. The main focus was to build a model to identify the healthiness of the lightning surge arresters based on their temperature profiles. Leakage current, insulation resistance and finite element method (FEM) based simulations were considered to validate the healthiness of the arresters. Using this model, it can be visualized whether the surge arrester condition is acceptable, only using a single thermal image of the arrester as an input. Even though, an arrester islocated in good condition region of the proposed model, the distance to the decision boundary indicates how close that arrester to be in unhealthy region.

Keywords: Thermal Imaging, Principal Component Analysis, Support Vector Machine, Leakage Current, Finite Element Method

1. Introduction

Lightning surge arresters play a crucial role in protecting electrical power systems from transient over-voltages caused by lightning strikes. These arresters, which consist of ZnO/SiCarrester material housed by insulation of silicon rubber(SIR)/porcelain, are essential in maintaining the reliability and stability of power system networks, particularly in regions frequently prone to lightning [1,2]. Therefore, early detection of potential issues of arresters can prevent catastrophic failures, reduce maintenance costs, and enhance the overall reliability of the power distribution system. For that, effective condition monitoring is imperative to detect any deterioration or failure in their performance.

During the monsoon seasons, Sri Lanka experiences a significant increase in lightning activity, leading to a higher incidence of surge arrester malfunctions. Records indicate that such malfunctions frequently result in damage to the distribution power transformers. In addition, the resulting surges can flow to the secondary side of the transformer [3], exposing customer energy meters, protective devices such as RCCB, and appliances at risk of damage due to lightning-induced over-voltages. This highlights the critical importance of effective condition monitoring for 33kV lightning surge arresters to prevent these failures and protect both the distribution network and end-user appliances and protective devices. Assessing the condition of the internal materials of surge arresters directly is not feasible by visual scrutiny. However, with ageing or malfunctioning of arresters, the leakage current inside the arrester increases, leading to a rise in temperature due to Joule heating. Since there are thousands of arresters at the 33 kV distribution network, conducting laboratory tests or off-line field tests for leakage currents in all arresters is also impractical. Therefore, monitoring and analysing the temperature of the arresters presents an effective alternative method to detect leakage current values.

Eng. R.S. Illesinghe, AMIE(SL), B. Sc. Eng. (Hons) (Peradeniya), SIEEE, Instructor in Electrical and Electronic Engineering, SLIIT.Email:raveeshaillesinghe@gmail.com
https://orcid.org/0009-0005-3661-5212
Eng. N.N.K. Paranavithana, AMIE(SL), B. Sc. Eng. (Hons) (Peradeniya), SIEEE, Electrical Engineer, LTL Holdings (Pvt) Ltd. Email:nisalnavodya98@gmail.com
https://orcid.org/0009-0005-1327-7636
Eng. (Prof.) M.A.R.M. Fernando, C. Eng, FIE(SL), B. Sc. Eng. (Hons) (Peradeniya), Lic. Tech (KTH), PhD (Chalrmers), SMIEEE, Professor at SLIIT, and University of Peradeniya. Email:manjula@ee.pdn.ac.lk
https://orcid.org/0000-0002-4587-4890
Eng. (Dr.) W.L. Abeygunasekara, AMIE(SL), B. Sc. Eng. (Hons) (Peradeniya), M.S. (Purdue), PhD(Peradeniya), Senior Lecturer at University of Peradeniya. Email:waranatha@eng.pdn.ac.lk
https://orcid.org/0000-0003-4349-5819

By observing temperature variations, it is possible to infer the condition of the arresters and identify those at risk of failure. This paper proposes an online thermal image-based simulator to identify the healthiness of lightning surge arresters based on their temperature profiles. The results were validated by laboratory conducted leakage current (LC), insulation resistance (IR) tests and FEM simulation results for energized 33 kV SIRhousedZinc Oxide surge arresters. The following sections describe on surge arrester condition monitoring methods, detailed methodologies used for the study, results of analysis and implications of findings.

2. Samples for Testing

According to the statistics of Meteorology Department of Sri Lanka, Kandy-Peradeniya area has a high keraunic level for lightnings [4]. Most of the lightning strikes occur during inter monsoon season from March to May and October to November. For this study, surge arresters were selected from Kandy district under the following different conditions.

2.1 Field-Energized Aged Surge Arresters

33 kV SIR insulated Zinc Oxide Surge arresters which were energized at 33 kV and having different ageing spans were taken into consideration. For example, Figure 1 shows a photograph and its thermal image of such surge arresters mounted on a 33 kV distribution transformer located at New Akbar Hostel premises of University of Peradeniya, captured on the 13th of September 2023.

Figure 1 – Photograph of Surge Arresters Connected to a 33 kV Transformer (Left) and Its Thermal Image (Right)

2.2 Laboratory-Tested Aged Surge Arresters

Field aged surge arresters were collected from CEB and they were brought to the high voltage (HV) laboratory of University of Peradeniya to measure the LC and IR. Samples were categorized according to the arcing and creepage distances (see Table 1) to calculate the applying voltage corresponding to electric stress applied for LC measurement match with 33 kV.

2.3 Reference Sample

As the reference sample, a brand-new arrester was chosen. Voltage stress was calculated according to the reference with a supply voltage of 20 kV. Table 1 shows the details of all the samples. Their creepage distances (LC path), arcing distances (lightning surge path) are included for comparison.

3. Condition Monitoring Methods

Lightning surge arresters can fail due to moisture ingress from sealing problems, aging of ZnO varistors, dust particles on the external surface, cracks on the insulation surface, and internal partial discharges [5]. There are both direct and indirect existing methods to monitor the conditions of lightning surge arresters [6]. Some of them are listed as follows.

3.1 Measuring Leakage Currents

This current is typically measured offline in a controlled laboratory environment, which can be challenging due to the large number of arresters in the field. Leakage current consists of both resistive and capacitive components [7]. The resistive component of the leakage current flows through the arrester's conductive path, representing the true power loss within the arrester. This component is influenced by the condition of the arrester's internal elements, such as the Metal Oxide Varistor (MOV) blocks. An increase in resistive leakage current typically indicates degradation or contamination of the MOV blocks, leading to high power losses and potential overheating. Monitoring the resistive component is critical for assessing the arrester's health and predicting its remaining service life. The capacitive component is primarily associated with the arrester's dielectric properties. This component is influenced by the arrester's design and the applied voltage but remains relatively stable under normal conditions. Changes in the capacitive leakage current is usually minor and less indicative of immediate issues compared to the resistive component. The contributions from resistive and capacitive currents are highlighted by the phase shift of voltage and current waveforms.

3.2 Measuring Insulation Resistance

This method assesses the integrity of the arrester's insulation by applying a 5 kV DC voltage and measuring the resulting resistance. In practice, IR measurements are taken at 1 minute and 10 minutes using a Megger meter and the polarization index (ratio between two IR values) is also taken.

Table 1 - Details of Field Energized Aged Samples and Laboratory-Tested Aged Samples

Sample Number	Colour	Number of Sheds	Installed Location	Estimated Age	Creepage Distance /(m)	Applied Voltage Stress /(kV/m)	Arcing Distance /(m)
F#01 F#02 F#03	Red	13	Eeriyagama CEB Customer Service Centre	Installed in 1999 (25 years)	-	-	-
F#04 F#05 F#06	Ash	13	Water Board of Peradeniya	Installed in 2021 (3 years)	*1.0	19.05	*0.5
F#07 F#08 F#09	Red	16	New Akbar Hostel, University of Peradeniya (UoP)	Installed in 2018 (6 years)	*1.21	15.75	*0.55
F#10 F#11 F#12	Ash	16	Seed Testing Centre, Gannoruwa Road, Kandy	Unknown	-	-	-
F#13 F#14 F#15	Red	16	Gorakadeniya Transformer, Kandy	Middle arrester was replaced in 2023 (1 year)	*1.21	15.75	*0.55
F#16 F#17 F#18	Red	16	Faculty of Engineering, UoP		*1.21	15.75	*0.55
L#00	Ash	13	(Reference)	(Brand-new)	0.95	21.05	0.37
L#01 L#02 L#03 L#04 L#05 L#06 L#07 L#08	Red	16	Samples were collected from Eriyagama Customer Service Centre	Removed in 2020 (4 years)	1.21		0.55
L#09 L#10 L#11	Ash	11		Unknown	0.9		0.55
L#12	Ash	13		Removed in 2020(4years)	1.0		0.49
L#13	Ash	12		Unknown	0.97		0.37
L#14 L#15 L#16 L#17 L#18 L#19	Red	16		Removed in 2019 (5 years)	1.21		0.55
L#20 L#21 L#22 L#23 L#24	Ash	13		Removed in 2020 (4 years)	1.0		0.37
L#25 L#26	Ash	13		Unknown	0.98		0.38
L#27	Ash	12		Unknown	0.97		0.31

*Creepage and arcing distances for field-energized samples were taken from samples available at CEB

A high insulation resistance indicates good insulation quality, while a low resistance indicates deterioration, contamination, or moisture ingress within the arrester [8].Regular IR testing helps to identify potential failures early, allowing for timely replacement.

3.3 Third Hamonic Measurement

Measuring the third harmonic of leakage current is an advanced technique in condition monitoring of surge arresters [9]. The third harmonic component arises primarily from the nonlinear characteristics of the MOV blocks within the arrester. Analysing this harmonic allows for the detection of subtle changes in the arrester condition that may not be apparent through direct current measurements alone. An increase in the third harmonic can indicate aging, degradation, or contamination of the MOV blocks. By taking Fourier transform of LC waveform third harmonic content can be estimated.

3.4 Infrared Imaging

This allows for the detection of temperature variations caused by internal power losses. When MOV blocks inside the arrester degrade, they generate heat that elevates the surface temperature [10]. Infrared thermography (430 THz to 300 GHz), using thermal cameras, captures this emitted radiation to provide a temperature profile. This non-contact method is advantageous for its safety and efficiency. Comparing thermal profiles across different arresters helps to identify significant anomalies, facilitating early detection of potential failures.

4. Methodology

Several field work and laboratory activities were done prior to building the thermal image simulator. The scope of the research was defined as the block diagram in Figure 2.

4.1 Field Investigation of Field-Energized Aged Surge Arresters

33kV surge arresters which are energized in the distribution network were selected atsix different locations; Transformer at Eeriyagama CEB Customer Service Centre, Main Transformer of Waterboard - Peradeniya, Transformer near New Akbar Hostel-University of Peradeniya, Transformer at Seeds Testing Centre-Gannoruw Road, Gorakadeniya Distribution Transformer and Transformer at Faculty of Engineering, University of Peradeniya. Both visual and thermal inspections were done for all the collected samples. Surge arrester in Figure 3 was inspected and there were no visual defects but a significant outlier was detected from the thermal inspection which can be observed as a red spot in the thermal image.

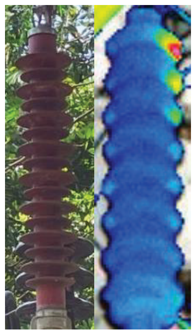

Figure 3 – Visual (Left) andThermal Inspection (Right) of a Surge Arrester Located in Gorakadeniya Distribution Transformer

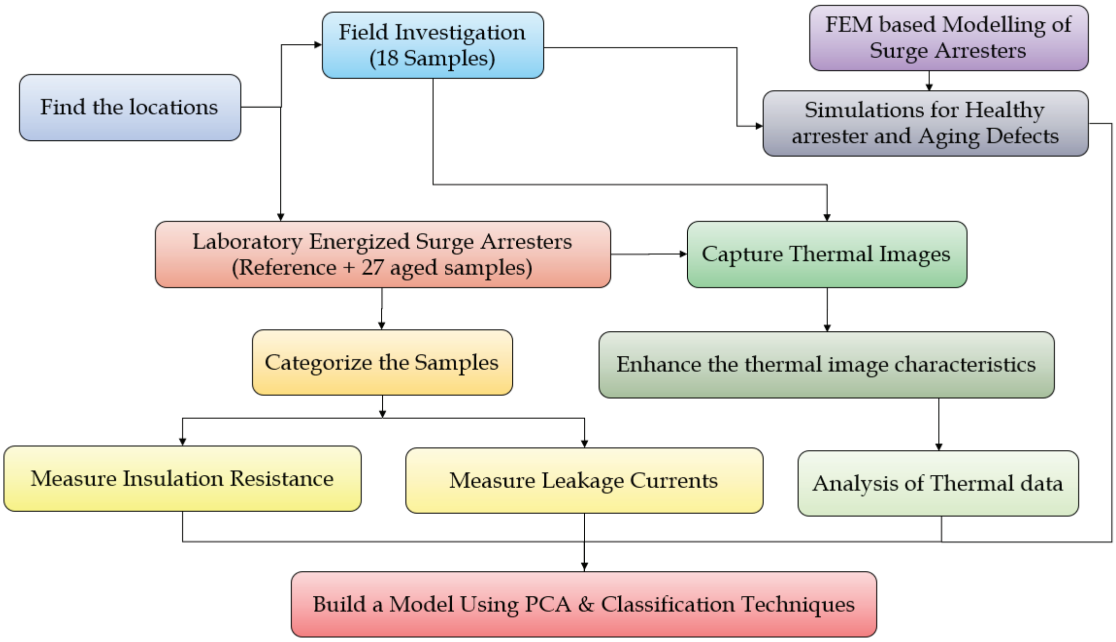

Figure 2 – Block Diagram of Methodology

Using image processing techniques aided with FLUKE SmartView software (refer section 4.2.3), temperature variation along the creepage distance is plotted as in Figure 4. The resulting plots were compared with the reference and with the finite element method results which will be discussed in Chapter 4.3 to classify them as good/bad conditions.

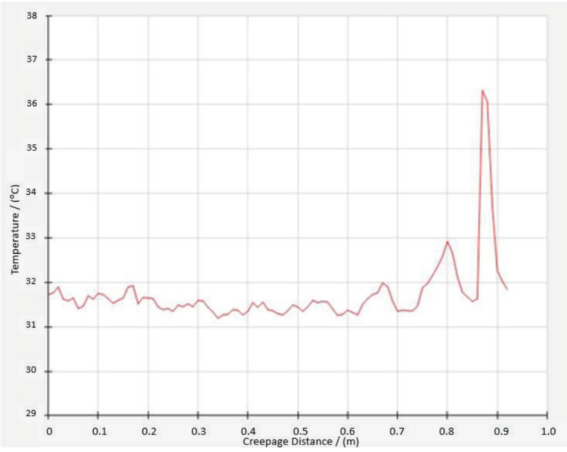

Figure 4 – Variation of Temperature along Creepage Distance of Considered Surge Arresterin GorakadeniyaTransformer

4.2 Laboratory Experiments for Field Aged Surge Arresters

As mentioned in Chapter 2.2, voltage is applied to the field aged surge arresters in the high voltage laboratory. Meanwhile, leakage current was measured and an infrared thermal image was captured simultaneously. Insulation resistance was measured using a 5 kV DC megger meter prior to energizing the arrester.

4.2.1 Leakage Current

A circuit was designed as shown in Figure 5 to measure the leakage current [11]. The circuit is connected through a HVAC transformer and a capacitive divider through secondary side rather than connecting directly to the primary side with 400 V three phase supply. The reasons for these selections are to encounter phase shifts of the transformer and ensure accurate measurement, to reduce interferences of high frequency components or noise, to change the voltage levels and for safety by isolating test object and the measuring circuit from the voltage source. 1.5 m long co-axial cable having a characteristic impedance of 50 Ω was used. The voltage through the divider is to ensure any phase shifts. The leakage current of the test object was measured through the measuring resistor of 1 kΩ high voltage resistor.The designed circuit was implemented and leakage current measurements were taken for all the samples as shown in Figure 6.

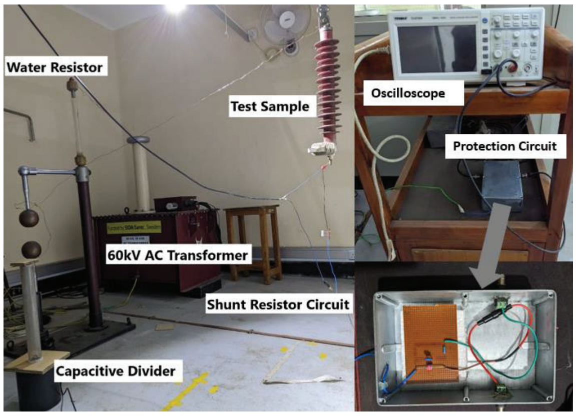

Figure 6 – Implemented Circuit in HV Laboratory

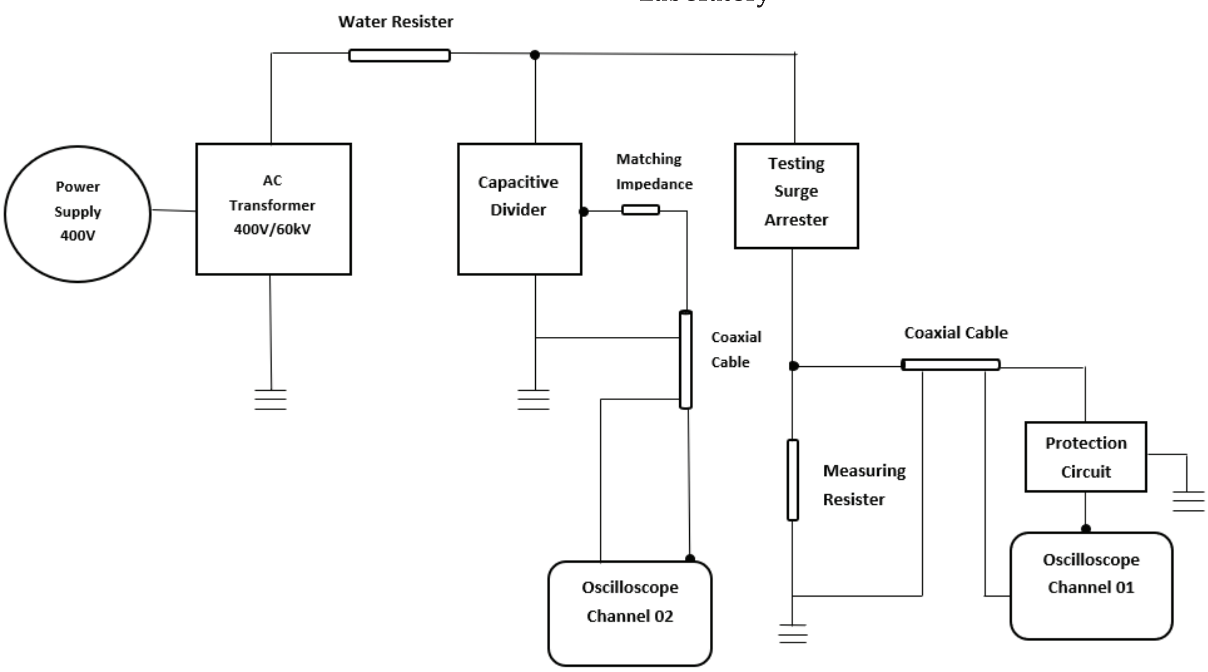

Figure 5 – Leakage Current Measuring System

For example, Figure 7 is the waveform of the oscilloscope for sample number 18. Voltage waveform through the divider is indicated in yellow and voltage waveform through the 1 kΩ shunt resistor is indicated in blue.

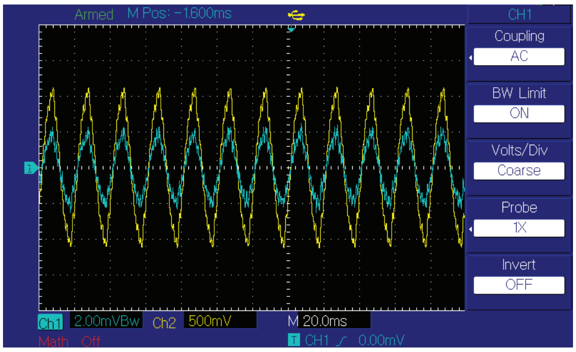

Figure 7 – Waveform of Sample No.18

For all the samples, any phase shift was not observed. The current waveforms are nearly sinusoidal indicating a negligible third harmonic component. Table 2 gives the resistive leakage current measurements for all the samples.

4.2.2 Insulation Resistance

Two terminal method was used to consider both surface and arrester insulation. Table 2 also shows the 1-minute IR, 10-minute IR and the polarization index for all 28 samples. But for this study, only 1 – minute IR is considered.

4.2.3 Thermal Data Extraction

In Sri Lanka, Ceylon Electricity Board has recommended on using FLUKE thermal cameras for the visual inspections because of their quality imaging and ideal features [12]. For this study, FLUKE Ti450 imager was used as the thermal imager because of its high resolution and minimum focus distance. Some of the key features addressed by the FLUKE Ti450 imager [13] which are ideal for the inspection requirement of this study are mentioned in Table 3. During the field inspection and the laboratory experiment, thermal images were captured. It is recommended to check the ambient temperatures while capturing, which is important for further analysis.

Table 2 – Resistive Leakage Current Measurementsand Insulation Resistance Measurements

Sample No.	Leakage Current / (µA)	IR with Guard Terminal / GΩ		Polarization Index
		1-min	10-min	
L#00(reference)	0.3	170	182	1.07
L#01	0.4	52	62	1.19
L#02	0.8	60	73	1.22
L#03	0.8	74	89	1.2
L#04	0.6	53	69	1.31
L#05	0.4	102	110	1.08
L#06	0.4	104	119	1.15
L#07	0.6	76	80	1.05
L#08	0.4	117	126	1.07
L#09	0.4	92	110	1.2
L#10	0.7	96	104	1.08
L#11	0.3	93	115	1.23
L#12	0.4	104	109	1.05
L#13	0.3	16.7	19.2	1.15
L#14	0.4	133	155	1.17
L#15	0.3	88	95	1.08
L#16	0.3	145	155	1.07
L#17	0.4	113	126	1.11
L#18	1.8	0.16	0.195	1.22
L#19	0.4	95	107	1.12
L#20	0.3	505	507	1.01
L#21	0.3	52.2	68.5	1.31
L#22	0.3	84.5	106	1.25
L#23	0.3	112	136	1.21
L#24	0.4	10.1	14.2	1.41
L#25	1.2	0.482	0.494	1.02
L#26	0.4	11.9	13.6	1.14
L#27	0.3	6.75	7.75	1.15

Table 3 - FLUKE Ti450 Key Features

Feature	Detail
Detector Resolution	320 x 240
Infrared Resolution	76,400 pixels
Advance Manual Focus	Yes
Temperature Range	-10 to 1500 °C
Accuracy	2 °C
On-screen Emissivity Correction	Yes
Minimum Focus Distance	Standard and Wide-Angle Lens – 15cm 2X and 4X telephoto Lens – 45cm
Auto Rescale	Yes
Software	FLUKE SmartView
Image file Formats	.bmp .jpeg .is2

The image properties were enhanced as in Figure 8 with two steps. Using a programming platform such as Open CV with a suitable programming language (Python was used for this study), image properties can be modified. Enlarging, filtering, segmentation & edge detection are some of the main features used for image processing part. As the next step, FLUKE SmartView software [14] is used to further modify the image. Thermal image processing step is very important because the accuracy and the effectiveness of the research outcome will depend on the quality of the thermal data. As the main goal is to extract accurate thermal data, the image feature quality should be maintained.

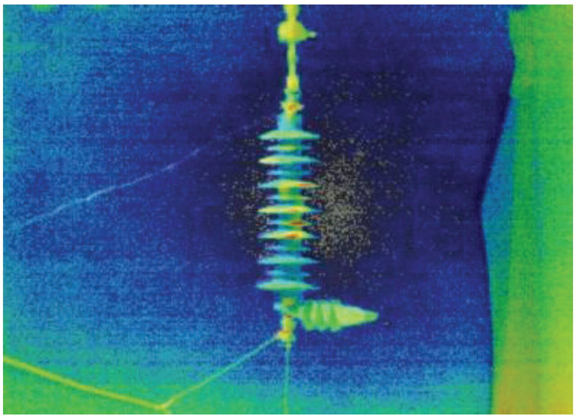

Figure 8 - Example of an Image Processed Thermal Image

After processing the image, thermal data can be extracted using the FLUKE Smart View software (Figure 9 is an overview of the FLUKE SmartView software interface.) which is a tool used for extracting thermal data from the thermal images and for analysing using various graphical illustrations. This software can give point wise temperature data through a desired direction along the object with an accuracy of

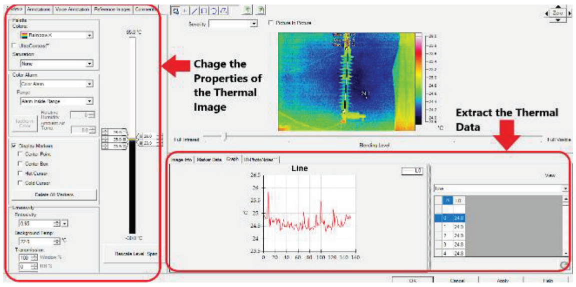

Figure 9 - FLUKE SmartView Software Interface

0.1 °C. Number of temperature points along a direction is varied according to the quality of the image.

The surge arrester was initially separated from the background of the thermal image and the thermal data of each point along the middle of the arrester was extracted because the internal current flow is maximum through the non-linear varistor blocks which are located along the centre line of the arrester. Temperature scale can be adjusted according to the required temperature range of the user. Moreover, various annotations can be used on the image for further analysis. This process was conducted for all the samples and data was exported into a data sheet for the analysis. The extracted data can be copied to any illustration tool and perform a graphical or a statistical analysis to see the variations in temperature of each surge arrester. Through this software, it is possible to extract line plots or 3D plots along the selected direction of an object as well.

For this study, it is required to mark the ambient temperature when imaging. According to Figure 10, the variation of temperature along the arrester material is stated. Hence, having the current ambient temperature is important to identify the deviations oftemperature of the arrester from the ideal scenarios. From these graphical interpretations of data, some key features of the arrester conditions can be clearly explained.

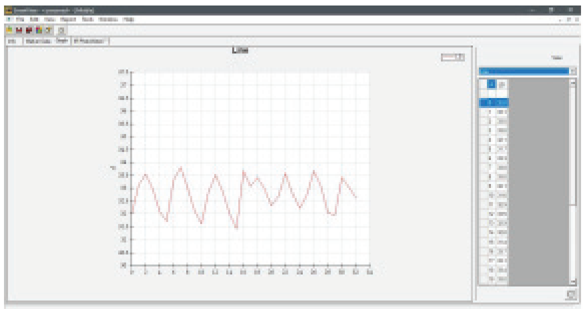

Figure 10 - Graphical Interpretation of Temperature Data in FLUKE SmartView Software

In some of the plots, unexpected high spikes can be seen which gives an understanding of an abnormal condition in the arrester material. The temperature difference along the inner and outer sheds can be clearly detected from the plots. Higher variations can be categorized as an unhealthy condition, with a more comprehensive study to be done. Some of the plots may have unexpected higher overall temperature variations which is also needed to be checked. As a result, it is important to compare these results with a plot of a normal temperature variation as a reference and address the various temperature changes of the other plots of the arresters. This will lead to accurate outcomes according to this study.

4.3 Simulation of Defects

Using FEM [1], a 33kV lightning surge arrester with ZnO varistor blocks and Silicon rubber housing insulation were modeled. Model was built in the region of pre-breakdown region according to the V-I Characteristics of ZnO. COMSOL Multiphysics V5.6 [15] was used as the FEM software with physics models of electrical currents and heat transfer in solids [16]. Material properties, boundry conditions, assumptions and mesh sizes wereobtained from literature [17]. Several common defects due to ageing that can be observed in the field were also modeled in the mentioned platform. Adding property changes to varistor blocks such as increasing electrical conductivity, adding an air cavity to SIR insulation and adding an artificial dust layer to make the surface of the sheds more conductive are made as some defects [18]. It was assumed that the air cavity is to be homogeneous for the simulation. Table 4 visualizes the results of surge arresters without any defects and with the mentioned defects at atmospheric temperature of 25 ^{0}C. According to the COMSOL modeling, it gave fair solutions with the field investigation observations with the means of reverseengineering to identify the worse conditions. Following are the results obtained.

- For a healthy arrester, temperature difference between inner and outer surfaces is about 0.5-2 °C.
- For a healthy energized arrester, temperature can be shifted approximately 1-2°C than the atmospheric temperature.
- A layer of contamination will affect to the temperature variation drastically.
- Property changes of varistor blocks will affect the temperature variations on the surface.

5. Proposed Model for Condition Monitoring

Using the above laboratory tests and FEM results, a total number of 46 surge arresters were categorized into two groups: healthy and not healthy. Accordingly, 10 samples were identified as not healthy. For laboratory tests, if the leakage current is greater than 1 μA or insulation resistance is less than 1 GΩ was considered as unhealthy conditions. From the whole set, 31 arresters were used to build the model and the rest was used to validate the model.

5.1 Dimension Reduction

Initially, the temperature values of each pixel along the centreline of the surge arrester were extracted. Since all the thermal images were taken at a 1m distance, there were 180 pixels along the arrester. However, consideration of 180 features for a large number of arresters is complex. Therefore, a linear dimensionality reduction technique named Principal Component Analysis [19] was used to reduce 180 parameters into two dimensions. According to Figure 11, the most dominant principal components were selected as PC1 and PC2 to map on a 2D plot.

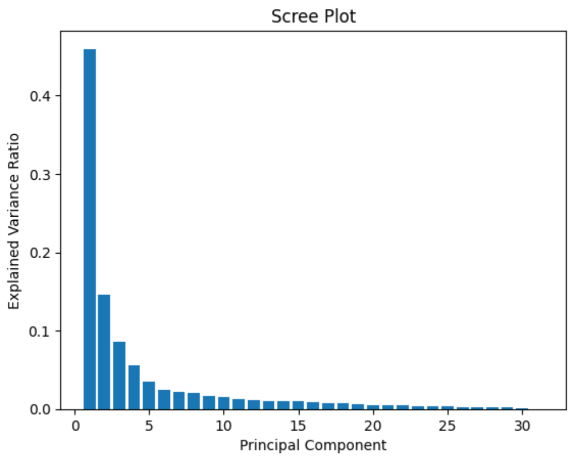

Figure 11 - Scree Plot ofFirst 30 Features of 180

With the selected dimensions of PC1 and PC2, the scatter plot was obtained for 31surge arresters.The scree plot shows that PC1 has a significant variance (about 0.475) compared to PC2 (about 0.15). The obtained scatter plot also shows similar behavior, i.e., PC1 varies from -15 to 25 whereas PC2 is -10 to -15 (Refer the Figure 12). Points related to healthy surge arresters are marked in blue and unhealthy surge arresters are marked in red in the scatter plot which is shown in Figure 12. It shows a clear separation between PCs of healthy and non-heathy samples by the decision boundary by a straight line.

Table 4 – Results of Finite Element Method

Description	Temperature Profile	Electrical Potential	Line Plot of Temperature
Healthy Surge Arrester	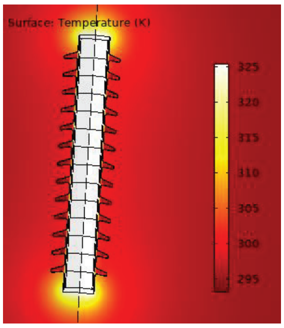	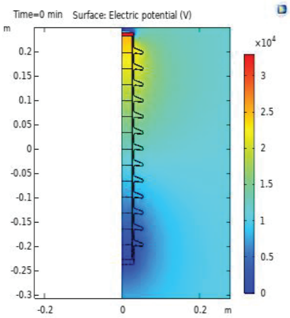	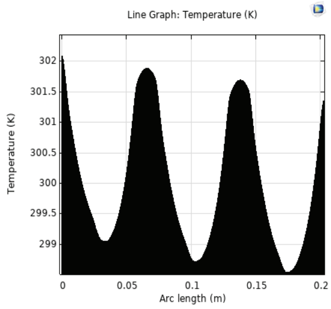
Electrical conductivity of varistor blocks is increased	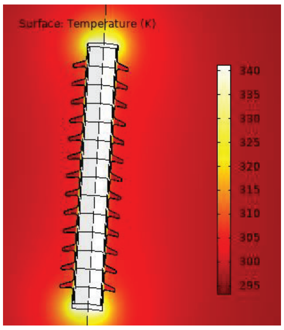	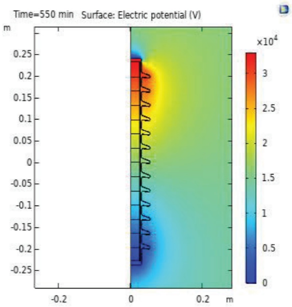	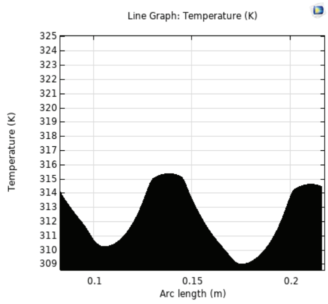
Artificial air cavity is added to the SiR insulation	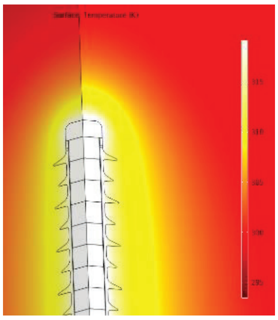	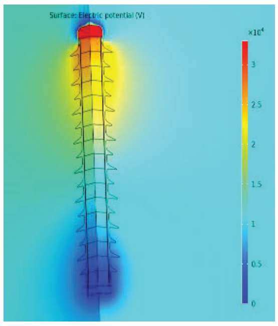	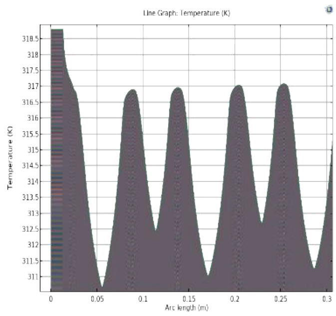
Artificial dust layer is added on the surface of the sheds	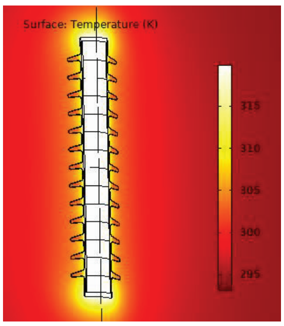	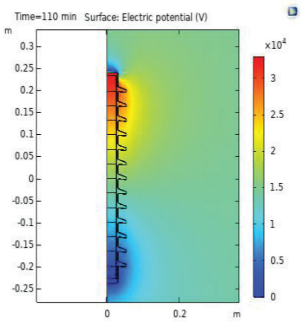	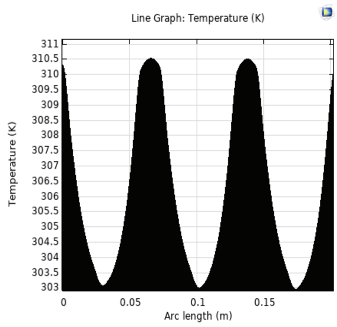

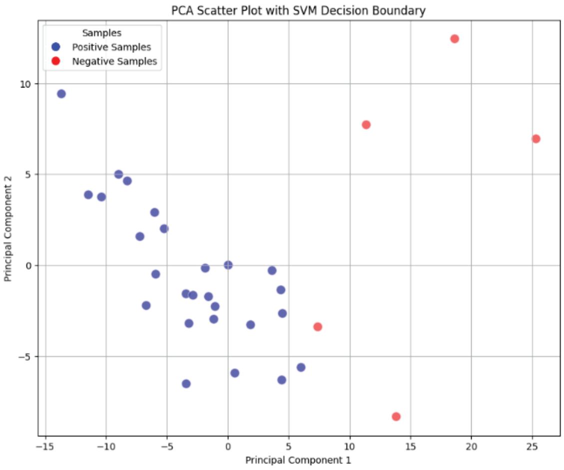

Figure 12 – Scatter Plot after Grouping

5.2 Support Vector Machine

To define the decision boundary hyperplane, support vector machine (SVM) was used [20]. In Figure 13, the decision boundary was drawn visualizing its equation. Accordingly, the decision boundary is defined as:

$$z = 0$$

$$\text{where, } z = -(PC1) - 2.58(PC2) + 12.78$$

Moreover, the perpendicular distance from a corresponding point in the scatter plot to the boundary line can be considered as a measurement of healthiness.

5.3 Classification

According to the built model, if the z value is less than zero it is considered as a healthy surge arrester. Otherwise, if the z value is greater than zero it is considered as an unhealthy surge arrester.

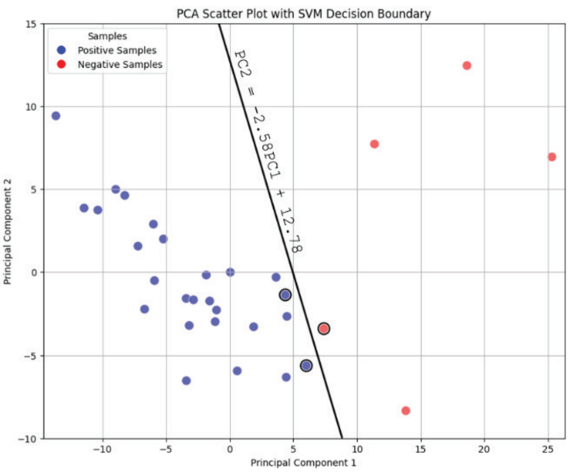

Figure 13 – Scatter Plot with Decision Hyperplane and Support Vectors

6. Validation of Results

Out of 46 samples, 15 surge arresters were used to validate this model. Figure 14 explains the results. Results of validation can be explained according to the confusion matrix in Table 5 as well. It is identified as giving 100% accurate results.

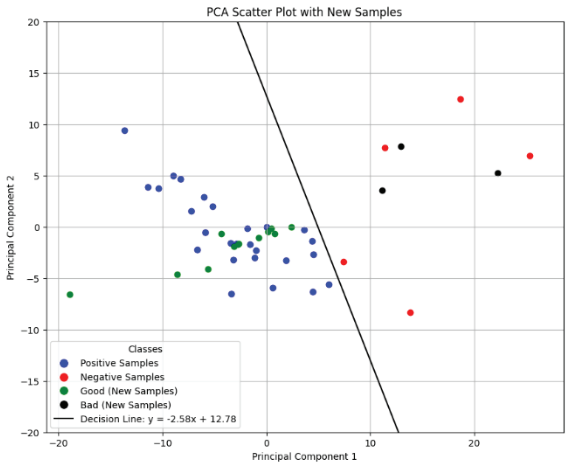

Figure 14 – Scatter Plot for Validation

Table 5 – Confusion Matrix of Results of Validation

		Actual Condition	
		Healthy	Not Healthy
Predicted Condition	Healthy	12	0
	Not Healthy	0	3

7. Conclusion

Surge arresters may age over time during their service, resulting in increased internal and surface leakage currents. Thermal images of such surge arresters highlighted by the arrester surface temperature profile indicate such increased leakage currents. The captured thermal images of the tested aged arresters are in agreement with measured leakage currents and insulation resistance values. Healthy and different aged scenarios such as aged varistors, air cavities and contaminated arrester surfaces can be simulated by FEM-based models based on the recorded thermal images. Analysis of 46 arrester samples showed that the overall information of thermal images highlighted by

180 dimensions could effectively be represented by the first two principal components in PCA. The proposed 2D Principal Components and SVM-based method offers an efficient, online condition assessment technique without disconnecting arresters from the power system, requiring only thermal images. This model can effectively detect broken, malfunctioning, or unhealthy 33kV ZnO surge arresters in distribution transformers and identifies samples near the decision boundary for continuous monitoring, achieving 100% accuracy with the tested 15 samples by the confusion matrix. Furthermore, the most precise decision boundary can be improved by increasing the number of arrester samples in the proposed PCA model.

Acknowledgment

The authors would like to express their gratitude to electrical engineers and technicians at Ceylon Electricity Board for their assistance for the field work.

References

1. Kuffel, E., Zaengl W. S. and Kuffel, J., *High Voltage Engineering Fundamentals,* Elsevier, 2000, Chapter 4, pp 246-253, and Chapter 8, pp 500-505.

2. Lucas, J. R., *High Voltage Engineering*, University of Moratuwa - Sri Lanka, 2001, Chapter 10.5.2, pp 174-175.

3. Fernando, M. A. R. M. and Cooray, V., "Lightning Surges at Distribution Transformer Secondary", *5th International Conference on Industrial and Information Systems(ICIIS)*, 2010, pp 532-537.

4. Premalal, K. H. M. S. and Kumarasinghe, N., "Community Base Vulnerability Mapping for Lightning Strikes in Sri Lanka", *Sri Lanka Journal of Meteorology*, Vol 1, 2015 December, pp 72-79.

5. Henderson, S., "Investigating Causes of Surge Arrester Failures'', [online] Power and Cables, (2021), Available at: https://www.powerandcables.com/investigating-causes-of-surge-arrester-failures/

6. Behnam, R., Darvishi, A., Rahman, D. and Hamid, R. S., "A Survey of Diagnostic and Condition Monitoring of Metal Oxide Surge Arrester in the Power Distribution Network", *Energies*, Vol. 15, Issue 21, 2022, pp 8091-8109.

7. Olesz, M., Litzbarski, L. S. and Redlarski, G., "Leakage Current Measurements of Surge Arresters", *Energies,* Vol. 16, Issue 18, 2023, pp 6480-6509.

8. James, R. E. and Su, Q., "Condition Assessment of High Voltage Insulation in Power System Equipment", *IET Power and Energy Series*, Vol. 53, 2008, pp 83-85.

9. Metwally, I. A., Eladawy, M. and Feilat, E. A., "Online Condition Monitoring of Surge Arresters Based on Third-Harmonic Analysis of Leakage Current", *IEEE Transactions on Dielectrics and Electrical Insulation*, Vol. 24, No. 4,2017 August, pp 2274-2281.

10. Novizon, N., Malek, Z. A., Bashir, N. and Asilah, N., "Thermal Image and Leakage Current Diagnostic as a Tool for Testing and Condition Monitoring of ZnOSurge Arrester", *Journal Teknologi*, Vol 64, No.4, 2013, pp 2180-3722.

11. Khavari, A. H., Munir, A. and Zulkurnain A. M., "Circuit-Based Method for Extracting the Resistive Leakage Current of Metal Oxide Surge Arrester", *Bulletin of Electrical Engineering and Informatics*, Vol. 9, No. 6, 2020, pp 2213-2221.

12. CEB Specification on Thermal Imaging and Measuring Devices (2018) Available at: https://www.ceb.lk/front_img/specifications/1540279643THERMAL_IMAGING_AND_MEASURING_DEVICES.pdf.

13. Fluke Ti450 Thermal Imagers User's Manual. (2013) Available at: https://www.instrumart.com/assets/Ti200through480-manual.pdf.

14. Fluke SmartView® IR Analysis reporting software and mobile app. (n.d.). Fluke. https://www.fluke.com/en/product/fluke-software/fluke-smartview-ir-mobile.

15. COMSOL Multiphysics Reference Manual. Available at:https://doc.comsol.com/6.0/doc/com.comsol.help.comsol/COMSOL_ReferenceManual.pdf

16. Ranaweera, O., Edirisinghe, T., Dhananjaya D., Fernando, M. A. R. M and Abeygunasekara, W. L., "FEM Based Modelling and Reliability Analysis of Lightning Protection in Anuradhapura Stupas with Installed Lightning Protection Systems", *Institute of Engineers, Sri Lanka, Transactions 2020 – part B*, Session 01.

17. Aibangbee, J. O., and Ikheloa, S. O., "Modelling and Evaluation of Leakage Current Behaviour of Metal oxide Surge Arresters under Various Applied Voltages and Polluted Conditions", *The International Journal of Engineering and Science (IJES)*, Vol. 8, Issue 9, Series 1, pp 11-20.

18. Christos, A. C., Vasiliki, V., Georgios, P., Lambros, E. and George, M., "Adjusting the Parameters of Metal Oxide Gapless Surge Arresters' Equivalent Circuits Using the

Harmony Search Method”, *Energies*, Vol 10, Issue 12, 2017, pp 2168-2179.

19. Jolliffe, I. T., “Principal Component Analysis: A Beginner’s Guide — I. Introduction and Application”, *Weather*, Vol. 45, 1990, pp 375–382.

20. Jakkula, V., "Tutorial on Support Vector Machine (SVM)", School of EECS, Washington State University, Vol. 37.2.5, 2006.